

# Bandgap engineering in an epitaxial two-dimensional honeycomb $\text{Si}_{6-x}\text{Ge}_x$ alloy

A. Fleurence,\* Y. Awatani, C. Huet, S. M. Wallace, T. Yonezawa, and Y. Yamada-Takamura  
*School of Materials Science, Japan Advanced Institute of Science and Technology,  
1-1 Asahidai Ishikawa 923-1292, Japan*

F. B. Wiggers

*MESA+ Institute for Nanotechnology, University of Twente,  
7500 AE Enschede, The Netherlands<sup>†</sup>*

## Abstract

In this Letter, we demonstrate that it is possible to form a two-dimensional (2D) silicene-like  $\text{Si}_5\text{Ge}$  compound by replacing the Si atoms occupying on-top sites in the planar-like structure of epitaxial silicene on  $\text{ZrB}_2(0001)$  by deposited Ge atoms. For coverages below  $1/6$  ML, the Ge deposition gives rise to a  $\text{Si}_{6-x}\text{Ge}_x$  alloy (with  $x$  between 0 and 1) in which the on-top sites are randomly occupied by Si or Ge atoms. The progressive increase of the valence band maximum with  $x$  observed experimentally originates from a selective charge transfer from Ge atoms to Si atoms. These achievements provide evidence for the possibility of engineering the bandgap in 2D SiGe alloys in a way that is similar for their bulk counterpart.

---

\* antoine@jaist.ac.jp

<sup>†</sup> Current address: ASML Netherlands B. V., De Run 6501, 5504 DR Verdhoven, The Netherlands

Alloying materials with similar structures and miscible elements is of great interest for a wide range of applications as it allows for adjusting various parameters to values which can not be achieved with elemental materials or compounds. This versatility is well exemplified by the engineering of the bandgap of semiconducting alloys which makes possible the fine tuning of the wavelength of solid-state lightings by controlling the alloys composition. With the continuous efforts to scale down the dimension of elementary bricks of electronic devices, the fabrication of low-dimensional alloys, including two-dimensional (2D) materials, became a technologically important challenge [1] as it was for bulk semiconducting materials in the past. Alloying semimetallic graphene, with its isomorphic wide-bandgap analogue h-BN which would have permitted to set the value of the bandgap of a 2D h-BNC alloy in a wide energy range, was however found to be hindered by the low miscibility of the two materials resulting in a phase segregation [2]. In contrast, ternary and quaternary alloys of transition metal dichalcogenide could be synthesized successfully [3–7] and the tunability of the optical bandgap was demonstrated. Among the 2D materials experimentally fabricated, silicene, a 2D honeycomb lattice of Si atoms, has the particularity to allow for continuing scaling down the Si-based nanoelectronics [8]. Thorough efforts were put into evaluating methods for tuning the electronic properties of silicene including doping [9, 10], or the adsorption of adatoms or molecules [11–13]. Alloying free-standing forms of silicene and germanene, its Ge analogue, investigated by first principles calculations [14–16] suggested that such 2D hexagonal SiGe alloys are stable and various parameters including the lattice parameter or the spin-orbit gap open in the Dirac cones were found to be tunable with the Si:Ge ratio while the non-triviality of the band structure is preserved.

In this Letter, we report the realization of a 2D SiGe epitaxial alloy fabricated by depositing Ge on silicene on zirconium diboride ( $\text{ZrB}_2$ ) films grown on Si(111) [17]. Furthermore, we investigated the possibility of engineering its bandgap in a way similar to bulk SiGe alloys. Epitaxial silicene sheets were prepared by annealing  $\text{ZrB}_2$  thin films epitaxially grown on Si(111) [18, 19] in ultrahigh vacuum (UHV). The deposition of Ge on silicene was realized by means of a Knudsen cell implemented in each of the UHV systems used for these experiments. The Ge flux, calibrated in each of these systems by depositing Ge on a Si(111) substrate, was in the  $0.09 - 0.12 \text{ ML}\cdot\text{min}^{-1}$  range (1 monolayer (ML) refer to the density of atoms in epitaxial silicene on  $\text{ZrB}_2(0001)$ :  $1.73 \times 10^{15} \text{ at}\cdot\text{cm}^{-2}$ ). Scanning tunneling microscopy (STM) was performed at room temperature. Photoemission spectroscopy exper-

iments were conducted at beamline BU06 of UVSOR. Core-level spectra in normal emission and angle-resolved photoemission spectroscopy (ARPES) spectra were recorded at room temperature and at 20 K, respectively. The respective energy resolutions as estimated from the broadening of the Fermi edge are 35 and 10 meV.

DFT calculations within a generalized gradient approximation (GGA) [20, 21] were performed using the OPENMX code [22] based on norm-conserving pseudopotentials generated with multireference energies [21] and optimized pseudoatomic basis functions [22]. The two input structures consist of  $(2 \times 2)$  ZrB<sub>2</sub>(0001) slabs made of 8 Zr and 7 B layers terminated on both face respectively by silicene or Si<sub>5</sub>Ge layers. A 42 Å vacuum space is separating the slabs. For Zr atoms, a s3p2d2 basis function i.e. including three, two, and two optimized radial functions allocated respectively to the s, p, and d orbitals. For Si, Ge and B atoms, s2p2d1 basis functions were adopted. A cutoff radius of 7 Bohr was chosen for all the basis functions. A regular mesh of 220 Ry in real space was used for the numerical integrations and for the solution of the Poisson equation. A  $(5 \times 5 \times 1)$  mesh of k points was used. For geometrical optimization, the force on each atom was relaxed to be less than 0.0001 Hartree/Bohr. In order to take into account the strength of translational symmetry breaking, the spectral weight as derived from the imaginary part of the one-particle Kohn-Sham Green function, was unfolded to the Brillouin zone of the "one-Si-atom unit cell" [23] following a method described in Ref. [24].

Silicene crystallises spontaneously on ZrB<sub>2</sub>(0001) in a so called "planar-like" ( $\sqrt{3} \times \sqrt{3}$ )-reconstructed structure [23, 25] adopted by several forms of epitaxial silicene [26–28]. This structure fits with the  $(2 \times 2)$  unitcell of ZrB<sub>2</sub>(0001) in such a way that  $a_{Si} = \frac{2}{\sqrt{3}}a_{ZrB_2}$ , where  $a_{ZrB_2}$  (3.178 Å) and  $a_{Si}$  (3.65 Å) are the lattice parameters of unreconstructed silicene and ZrB<sub>2</sub>(0001), respectively. The Figs. 1.(a) and (b) show the details of the planar-like structure as the result of optimization in DFT calculations. In this structure, two, three and one Si atoms are respectively sitting on hollow, bridge and on-top sites of the Zr-terminated thin films. All of the Si atoms but one are laying 2.3 Å above the topmost Zr layer whereas the Si atoms sitting on the on-top sites visible in STM images are protruding at 3.9 Å. As shown in the STM image of Fig. 1.(c), the deposition of 0.05 ML Ge on silicene turns the domain structure of the pristine silicene sheet [18, 29] into a single domain in a way similar to the deposition of silicon[30]. However, in contrast to silicon atoms, the deposition of Ge

atoms results in a contrast between the protrusions, observed for all scanning conditions, and most visible for a bias voltage of 1.0 V, which suggests that some Ge atoms substituted Si protruding atoms. As this Ge coverage is beyond that required to fully turn the domain structure of silicene into a single-domain (0.03 ML) [30], the excess of atoms results locally in the formation of bilayer silicon islands [31] like the one shown in the inset of Fig. 1.(c). These islands are rare and distant (few hundreds of nanometers from each others).

The Fig. 1.(d) shows a photoemission spectrum recorded with a photon energy of  $h\nu=80$  eV in the region of the Zr4p and Ge3d core-levels after deposition of 0.09 ML Ge. The fact that the Ge3d component can be fitted with a single pair of Lorentzian functions, points out that the Ge atoms are incorporated into a single site, i.e. the on-top sites of the silicene lattice.

The Fig. 1.(d) presents such a planar-like structure after optimization by DFT, which appears to be essentially similar to that shown in Fig. 1.(a). The main difference is the length of the bonds between atoms of the on-top and bridges sites which increases from 2.37 Å to 2.47 Å. This distance is longer than that of the Si-Ge bonds measured in bulk SiGe alloys [32] or calculated for 2D hexagonal SiGe alloys [15]. The Ge atom is located 1.74 Å above the bottom Si atoms instead of 1.58 Å for the on-top Si atom in silicene which confirms that the taller protrusions must be assigned to Ge atoms. Fig. 2 shows the evolution with the Ge coverage of the silicene sheet as imaged by STM and photoemission spectra recorded in the Zr4p and Ge3d core-levels region. The number of protruding Ge atoms and the integrated intensity of the spectrum increase both linearly until a Ge coverage of 0.17 ML close to the density of protruding atoms in the planar-like structure (1/6 ML) is reached. One can deduce that below this coverage, Ge adatoms are fully incorporated into the silicene sheet and replace systematically protruding Si atoms in the planar-like structure. This shows that it is possible to fabricate a 2D  $\text{Si}_{6-x}\text{Ge}_x$  alloy with  $x$  being finely adjustable between 0 and 1 by depositing a controlled amount of Ge in this coverage range.

To determine the effect of the Ge atoms on the band structure of  $\text{Si}_{6-x}\text{Ge}_x$ , ARPES spectra were recorded for different values of  $x$  between 0 and 1. The Fig. 3 show spectra recorded with a photon energy of 45 eV in the region of the  $K$  point of the Brillouin zone of unreconstructed silicene where the valence band maximum (VBM) is located [18, 23, 25]. One can see that the top of the binding energy of the valence band  $E_{VBM}$  evolves steadily from  $E_{VBM}^{\text{Silicene}}=0.42$  eV for silicene to  $E_{VBM}^{\text{Si}_5\text{Ge}}=0.28$  eV for  $\text{Si}_5\text{Ge}$  whereas the bottom of the band

remains at a binding energy of 1.0 eV. The evolution of  $E_{VBM}$  with  $x$  is not linear and the fitting of  $\Delta E_{VBM} = E_{VBM}(x) - (E_{VBM}^{Silicene}x + E_{VBM}^{Si_5Ge}(1-x))$  with  $bx(1-x)$  gives a bowing parameter  $b$  of -135 meV (See inset of Fig. 3.(e)).

As shown in Figs. 4.(a) and (b), the difference in band structure between silicene and  $Si_5Ge$  observed experimentally is well reproduced by DFT calculations. The band structures were calculated for structures with a lattice parameter artificially increased by 5 % [23] to compensate the overestimation of the bandwidth caused by the GGA [33, 34]. In agreement with the experimental ARPES spectra, the VBM is shifted upwards by 90 meV (from 200 meV to 110 meV) whereas the bottom of the band remains at the same energy.

To evaluate the influence of the epitaxial strain on the band structure of the  $Si_{6-x}Ge_x$  alloy, the energy of the free-standing planar-like structures of silicene and  $Si_5Ge$  were calculated as a function of the lattice parameter of the unreconstructed silicene structure. To preserve the planar-like structure upon geometrical optimization in absence of the substrate, the 5 Si atoms of the bottom layers were forced to remain in the same plane. In contrast to the slight increase of the equilibrium lattice parameter found for free-standing 2D hexagonal SiGe alloy [15], the planar-like structures of silicene and  $Si_5Ge$  have the same equilibrium lattice parameter of 3.89 Å (Fig. 4.(c)), corresponding to a compressive strain of 6.2 % which suggests that any strain-induced effect on evolution of the band structure is negligible.

The good agreement between experimental and computed band structures allows for analysing further the nature of the effect of the Ge atoms. The Figs. 4.(f) and (g) show the respective contributions of on-top, hollow and bridges sites atoms, as indicated in Fig. 4.(d), to the band structures of epitaxial silicene and  $Si_5Ge$  plotted along the path indicated in Fig. 4.(e). For both structures, the valence band centered on the  $K$  point appears to originate from the Si atoms in the bridge sites, whereas the conduction band minimum (CBM) centered on the  $M$  point of the Brillouin zone of the unreconstructed silicene originates from the Si atoms of the hollow sites. One can observe that in contrast to  $E_{VBM}$ ,  $E_{CBM}$  the energy of the CBM does not vary much between the two structures. The comparison of the computed Mulliken charges carried by the different atoms (Table I) suggests that the on-top site Ge atoms are electron richer than the Si atoms in the same position, in agreement with the higher electronegativity of Ge (2.01) in comparison to that of Si (1.90). This induces an increase of the electron donation from the bridge site atoms which are the first neighbors of the on-top site atoms and thus become further positively charged. In contrast, the charge

carried by the hollow-sites atoms does not vary significantly. This selective charge transfer from on-top sites atoms to bridge sites atoms results in a progressive shift of  $E_{VBM}$  towards the Fermi level whereas  $E_{CBM}$  is fixed.

In conclusion, we experimentally demonstrated the possibility of fabricating an epitaxial silicene-like  $\text{Si}_5\text{Ge}$  compound by depositing a minute amount of Ge on silicene on  $\text{ZrB}_2(0001)$  thin films on  $\text{Si}(111)$ . For Ge coverages below  $1/6$  ML, the deposition gives rise to a  $\text{Si}_{6-x}\text{Ge}_x$  alloy based on the planar-like structure of epitaxial silicene in which the protruding sites are randomly occupied by Si or Ge atoms. The substitution of Si atoms by Ge atoms induces a shift of the VBM which allows for finely tuning the bandgap of the epitaxial  $\text{Si}_{6-x}\text{Ge}_x$  by controlling the amount of Ge atoms.

A.F. acknowledges financial support from JSPS KAKENHI Grant Number 26790005. F.B.W. acknowledges financial support from the Foundation for Fundamental Research on Matter (FOM, Project No. 12PR3054), which is part of the Netherlands Organization for Scientific Research (NWO). A part of this work was supported by the Joint Studies Program of the Institute for Molecular Science No. 203 (2016-2017) and No. 206 (2017-2018). This work was financially supported by Iketani Science and Technology Foundation. We are thankful to Dr. Hiroyuki Yamane (IMS) for his assistance at beamline BL6U of UVSOR.

- 
- [1] C. Ning, L. Dou, and P. Yang, *Nature Review* **2**, 17070 (2017).
- [2] L. Ci, L. Song, C. Jin, D. Jariwala, D. Wu, Y. Li, A. Srivastava, Z.-F. Wang, K. Storr, L. Balicas, F. Liu, and P. Ajayan, *Mat. Mater.* **9**, 430 (2010).
- [3] H.-P. Komsa and A. V. Krasheninnikov, *The Journal of Physical Chemistry Letters* **3**, 3652 (2012).
- [4] S.-H. Su, Y.-T. Hsu, Y.-H. Chang, M.-H. Chiu, C.-L. Hsu, W.-T. Hsu, W.-H. Chang, J.-H. He, and L.-J. Li, *Small* **10**, 2589 (2014).
- [5] Q. Fu, L. Yang, W. Wang, A. Han, J. Huang, P. Du, Z. Fan, J. Zhang, and B. Xiang, *Advanced Materials* **27**, 4732 (2015).
- [6] K.-A. N. Duerloo and E. J. Reed, *ACS Nano* **10**, 289 (2016).
- [7] S. Susarla, A. Kutana, J. A. Hachtel, V. Kochat, A. Apte, R. Vajtai, J. C. Idrobo, B. I. Yakobson, C. S. Tiwary, and P. M. Ajayan, *Advanced Materials* **29**, 1702457 (2017).
- [8] L. Tao, E. Cinquanta, D. Chiappe, C. Grazianetti, M. Fanciulli, M. Dubey, A. Molle, and D. Akinwande, *Nature Nanotechnology* **10**, 227 (2015).
- [9] H. Sahin and F. M. Peeters, *Phys. Rev. B* **87**, 085423 (2013).
- [10] R. Friedlein, A. Fleurence, J. T. Sadowski, and Y. Yamada-Takamura, *Applied Physics Letters* **102**, 221603 (2013).
- [11] M. Houssa, E. Scalise, K. Sankaran, G. Pourtois, V. V. Afanasev, and A. Stesmans, *Applied Physics Letters* **98**, 223107 (2011).
- [12] T. H. Osborn, A. A. Farajian, O. V. Pupyshcheva, R. S. Aga, and L. Lew Yan Voon, *Chemical Physics Letters* **511**, 101 (2011).
- [13] B. Huang, H. J. Xiang, and S.-H. Wei, *Phys. Rev. Lett.* **111**, 145502 (2013).
- [14] H. Şahin, S. Cahangirov, M. Topsakal, E. Bekaroglu, E. Akturk, R. T. Senger, and S. Ciraci, *Phys. Rev. B* **80**, 155453 (2009).
- [15] J. E. Padilha, L. Seixas, R. B. Pontes, A. J. R. da Silva, and A. Fazzio, *Phys. Rev. B* **88**, 201106(R) (2013).
- [16] R.-w. Zhang, C.-w. Zhang, S.-s. Li, W.-x. Ji, P.-j. Wang, F. Li, P. Li, M.-j. Ren, and M. Yuan, *Solid State Communications* **191**, 49 (2014).
- [17] A. Fleurence, Y. Yoshida, C.-C. Lee, T. Ozaki, Y. Yamada-Takamura, and Y. Hasegawa,

- Appl. Phys. Lett. **104**, 021605 (2014).
- [18] A. Fleurence, R. Friedlein, T. Ozaki, H. Kawai, Y. Wang, and Y. Yamada-Takamura, Phys. Rev. Lett. **108**, 245501 (2012).
- [19] Y. Yamada-Takamura, F. Bussolotti, A. Fleurence, S. Bera, and R. Friedlein, Applied Physics Letters **97**, 073109 (2010).
- [20] W. Kohn and L. J. Sham, Phys. Rev. **140**, A1133 (1965).
- [21] J. P. Perdew, K. Burke, and M. Ernzerhof, Phys. Rev. Lett. **77**, 3865 (1996).
- [22] T. Ozaki, Phys. Rev. B **67**, 155108 (2003).
- [23] C.-C. Lee, A. Fleurence, Y. Yamada-Takamura, T. Ozaki, and R. Friedlein, Phys. Rev. B **90**, 075422 (2014).
- [24] C.-C. Lee, Y. Yamada-Takamura, and T. Ozaki, Journal of Physics: Condensed Matter **25**, 345501 (2013).
- [25] C.-C. Lee, A. Fleurence, R. Friedlein, Y. Yamada-Takamura, and T. Ozaki, Phys. Rev. B **88**, 165404 (2013).
- [26] L. Chen, C.-C. Liu, B. Feng, X. He, P. Cheng, Z. Ding, S. Meng, Y. Yao, and K. Wu, Phys. Rev. Lett. **109**, 056804 (2012).
- [27] L. Meng, Y. Wang, L. Zhang, S. Du, R. Wu, L. Li, Y. Zhang, G. Li, H. Zhou, W. A. Hofer, and H.-J. Gao, Nano Letters **13**, 685 (2013).
- [28] T. Aizawa, S. Suehara, and S. Otani, The Journal of Physical Chemistry C **118**, 23049 (2014).
- [29] M. Nogami, A. Fleurence, Y. Yamada-Takamura, and M. Tomitori, Advanced Materials Interfaces **6**, 1801278 (2019).
- [30] A. Fleurence, T. G. Gill, R. Friedlein, J. T. Sadowski, K. Aoyagi, M. Copel, R. M. Tromp, C. F. Hirjibehedin, and Y. Yamada-Takamura, Applied Physics Letters **108**, 151902 (2016), <https://doi.org/10.1063/1.4945370>.
- [31] T. G. Gill, A. Fleurence, B. Warner, H. Prser, R. Friedlein, J. T. Sadowski, C. F. Hirjibehedin, and Y. Yamada-Takamura, 2D Materials **4**, 021015 (2017).
- [32] J. C. Aubry, T. Tylliszczak, A. P. Hitchcock, J.-M. Baribeau, and T. E. Jackman, Phys. Rev. B **59**, 12872 (1999).
- [33] D. E. Eastman, F. J. Himpsel, and J. A. Knapp, Phys. Rev. Lett. **44**, 95 (1980).
- [34] P. Haas, F. Tran, and P. Blaha, Phys. Rev. B **79**, 085104 (2009).

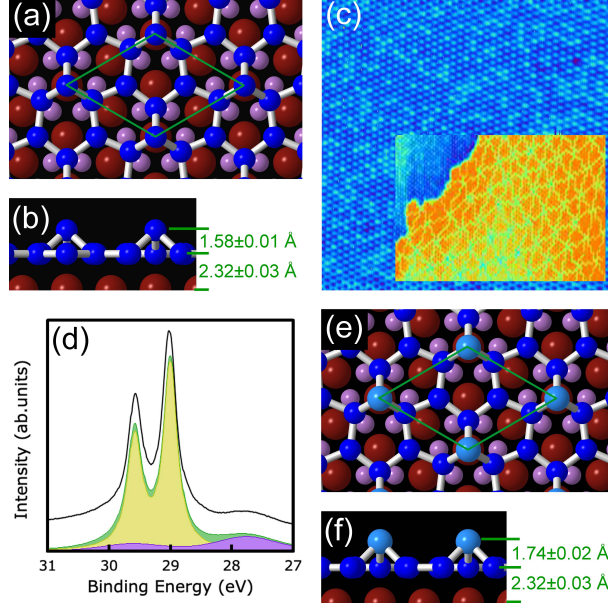


Figure 1. **Deposition of Ge on silicene on  $\text{ZrB}_2(0001)$ .** (a) and (b): Top- and side-views of the epitaxial planar-like structure of silicene on  $\text{ZrB}_2(0001)$  as determined by DFT calculations. Si, Zr and B atoms are respectively dark blue-, red- and purple-colored. The green rhombus indicate the  $(\sqrt{3} \times \sqrt{3})$ -reconstructed unitcell. (c): STM image ( $30 \text{ nm} \times 30 \text{ nm}$ ,  $V=1.0 \text{ V}$ ,  $I=100 \text{ pA}$ ) of epitaxial silicene after deposition of 0.057 ML Ge. The STM image ( $33 \text{ nm} \times 23 \text{ nm}$ ) in the inset shows the silicene-Ge alloy (top left) and Si bilayer islands side-by-side. (d): Photoemission spectrum recorded with  $h\nu=80 \text{ eV}$  in the Ge3d and Zr4p region after deposition of 0.090 ML Ge. The experimental spectrum is indicated by the black line. Yellow- and purple-filled curves are the contribution of Ge3d and Zr 4p core-levels determined by fitting and the green-filled curve is their sum. The full widths at half maximum are 270 meV and 290 meV respectively for the Ge3d<sub>3/2</sub> and Ge3d<sub>5/2</sub> peaks. (e) and (f): Top- and side-views of the structure of epitaxial  $\text{Si}_5\text{Ge}$  on  $\text{ZrB}_2(0001)$  as determined by DFT calculations. Si, Zr and B atoms are colored in the same way as in Figure (a) and Ge atoms are light blue-colored.

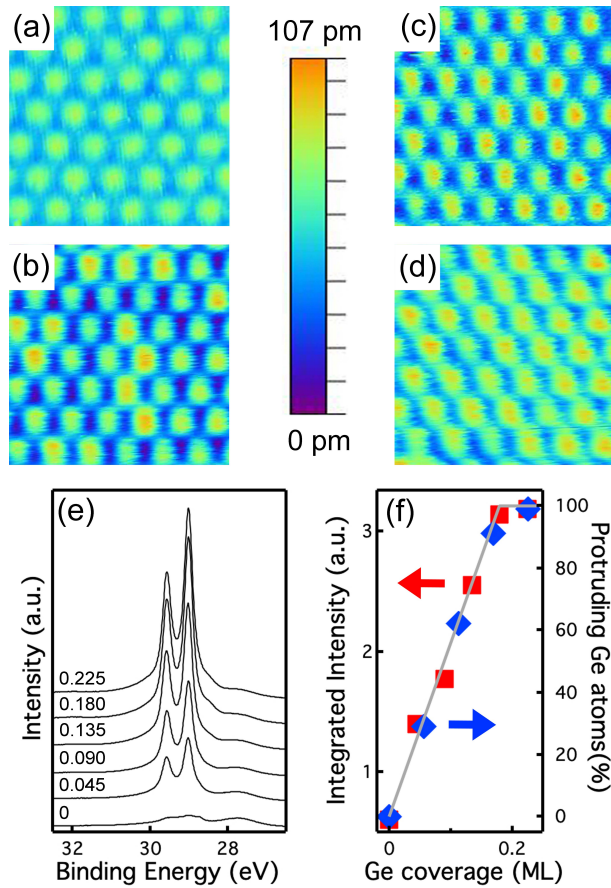


Figure 2.  $\text{Si}_{6-x}\text{Ge}_x$  alloy (a)-(d): STM images ( $4 \text{ nm} \times 4 \text{ nm}$ ,  $V=1.0 \text{ V}$ ,  $I=100 \text{ pA}$ ) after deposition of 0.030 ML Si, 0.057, 0.113, and 0.167 ML Ge. Their common color-coded z scalebar is shown. (e) Spectra recorded in the Ge 3d and Zr4p core-levels region recorded for different Ge coverage with a photon energy of 80 eV. (f): Integrated intensity of the photoemission spectra and percentage of protruding Ge atoms as functions of the Ge coverage.

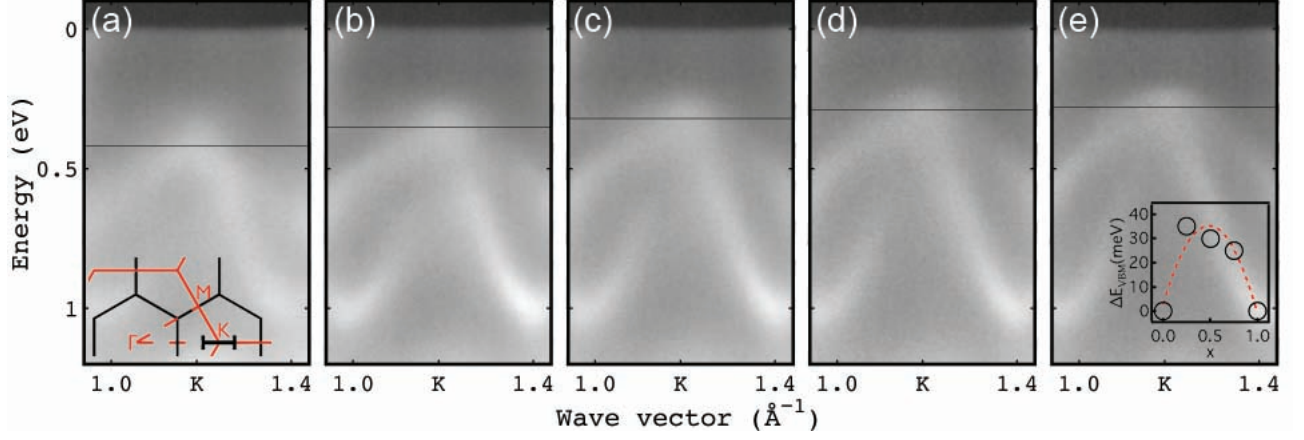


Figure 3. **Valence band of  $\text{Si}_{6-x}\text{Ge}_x$  alloy.** The inset of the figure (a) shows the region around the  $K$  point of the Brillouin zone of unreconstructed silicene in which the spectra were recorded. Brillouin zones of  $(\sqrt{3} \times \sqrt{3})$ -reconstructed and unreconstructed silicene are respectively indicated by black and red lines. (a)-(e): ARPES spectra recorded with a photon energy of  $h\nu=45$  eV on  $\text{Si}_{6-x}\text{Ge}_x$  alloys for  $x = 0, 0.25, 0.5, 0.75$  and  $1$ . The horizontal lines indicate  $E_{VBM}$ . The inset of Fig. (e) shows  $\Delta E_{VBM} = E_{VBM} - (E_{VBM}^{\text{Silicene}}x + E_{VBM}^{\text{Si}_5\text{Ge}}(1-x))$  as a function of  $x$ . Its fitting with  $bx(1-x)$  and  $b = -135$  meV is indicated by a dashed red line.

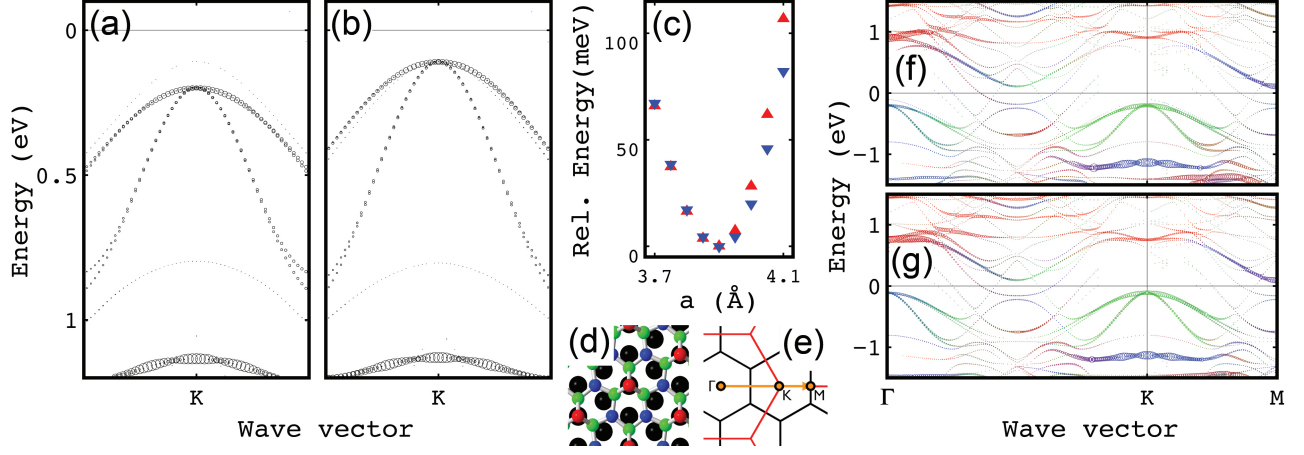


Figure 4. **Band structure of silicene and  $\text{Si}_5\text{Ge}$**  (a) and (b): Band structures of silicene and  $\text{Si}_5\text{Ge}$  in the region indicated in the inset of Fig. 3 (a). The spectral weight of the combined contribution of Si and Ge atoms is indicated by the size of the circles. (c): Lattice parameter-dependence of the energy per atom of free-standing planar-like structures of silicene (red) and  $\text{Si}_5\text{Ge}$  (blue). (d): Schematics of the planar-like structure on Zr-terminated  $\text{ZrB}_2(0001)$ . Zr, on-top, bridge and hollow atoms are respectively black-, red-, green- and blue-colored. (e): Schematics of the k-space. Black and red lines indicate the  $(\sqrt{3} \times \sqrt{3})$  and  $(1 \times 1)$  Brillouin zones of silicene. (f) and (g): Calculated band structures for silicene and  $\text{Si}_5\text{Ge}$  along the path indicated in Fig. (e). The contribution of the on-top, bridge and hollow sites atoms are respectively red-, green- and blue-colored in agreement with Fig. (d). The size of the circles represents the spectral weight of the combined contribution of Si and Ge atoms.

	On-top	Bridge	Hollow
Silicene	-0.052	0.083	-0.016
Si <sub>5</sub> Ge	-0.711	0.322	-0.020

Table I. Mulliken charges expressed in number of  $e^-$  calculated by DFT.